



Calibration of sealed HCl cells used for TCCON instrumental line shape monitoring

F. Hase¹, B. J. Drouin², C. M. Roehl³, G. C. Toon², P. O. Wennberg³, D. Wunch³, T. Blumenstock¹, F. Desmet⁴, D. G. Feist⁵, P. Heikkinen⁶, M. De Mazière⁴, M. Rettinger⁸, J. Robinson⁹, M. Schneider¹, V. Sherlock⁹, R. Sussmann⁸, Y. Té¹⁰, T. Warneke⁷, and C. Weinzierl⁷

¹Karlsruhe Institute of Technology (KIT), Institute for Meteorology and Climate Research (IMK-ASF), Karlsruhe, Germany

²Jet Propulsion Laboratory, Pasadena, CA 91109, USA

³California Institute of Technology, Pasadena, CA 91125, USA

⁴Belgian Institute for Space Aeronomy (BIRA-IASB), Brussels, Belgium

⁵Max Planck Institute for Biogeochemistry, Jena, Germany

⁶Finnish Meteorological Institute, Sodankylä, Finland

⁷Institute of Environmental Physics, University of Bremen, Germany

⁸Karlsruhe Institute of Technology (KIT), Institute for Meteorology and Climate Research (IMK-IFU), Garmisch-Partenkirchen, Germany

⁹NIWA, Lauder, New Zealand

¹⁰UPMC Univ. Paris06, Laboratoire de Physique Moléculaire pour l'Atmosphère et l'Astrophysique (LPMAA), UMR7092, CNRS, Paris, France

Correspondence to: F. Hase (frank.hase@kit.edu)

Received: 17 July 2013 – Published in Atmos. Meas. Tech. Discuss.: 5 August 2013

Revised: 8 November 2013 – Accepted: 12 November 2013 – Published: 16 December 2013

Abstract. The TCCON (Total Carbon Column Observing Network) FTIR (Fourier transform infrared) network provides highly accurate observations of greenhouse gas column-averaged dry-air mole fractions. As an important component of TCCON quality assurance, sealed cells filled with approximately 5 mbar of HCl are used for instrumental line shape (ILS) monitoring at all TCCON sites. Here, we introduce a calibration procedure for the HCl cells which employs a refillable, pressure-monitored reference cell filled with C₂H₂. Using this method, we identify variations of HCl purity between the TCCON cells as a non-negligible disturbance. The new calibration procedure introduced here assigns effective pressure values to each individual cell to account for additional broadening of the HCl lines. This approach will improve the consistency of the network by significantly reducing possible station-to-station biases due to inconsistent ILS results from different HCl cells. We demonstrate that the proposed method is accurate enough to turn the ILS uncertainty into an error source of secondary importance from the viewpoint of network consistency.

1 Introduction

The Total Carbon Column Observing Network (TCCON) is an international network of ground-based Fourier transform spectrometers that record direct solar spectra in the near-infrared (Wunch et al., 2011). The column-averaged abundances of the radiatively important greenhouse gases CO₂ and CH₄, as well as of a suite of other atmospherically significant trace gases (CO, N₂O, H₂O, HDO, and HF), are derived from these spectra. Investigating the global distribution of greenhouse gases such as CO₂ and CH₄ has, until recently, primarily relied on in situ measurements from surface station networks. Remote sensing of greenhouse gas columns (or vertically integrated mixing ratios) is thought to improve flux estimates since variations in the gas columns are more directly relatable to mass fluxes than surface concentration measurements (Keppel-Aleks et al., 2011). However, the gradients in column CO₂, for example, are small, requiring a precision and accuracy of < 1 ppm (< 0.25 %, Olsen and Randerson, 2004; Miller et al. 2007).

The instrumental requirements for the remote sensing of greenhouse gas columns from near-infrared solar spectra are therefore very exacting.

TCCON has developed strict data acquisition and analysis protocols to attempt to minimize differences between sites. Interferograms are obtained with similar instruments operated with common detectors and acquisition electronics. These interferograms are processed to spectra and then to retrieved products using a common pipeline processing system. Nevertheless, biases at individual sites and between sites can arise due to the behaviour of individual spectrometers, if not properly characterized. These differences may result from non-ideal instrument electronics (Messerschmidt et al., 2010) or a misalignment of the interferometer. The latter can change abruptly as a consequence of operator intervention or drift slowly due to mechanical degradation over the many months between visits to automated sites.

The next version of the TCCON data processing system will account for differences in the instrumental line shape (ILS) of the instruments. Mis-sampling of the interferograms will be removed as described by Dohe et al. (2013). ILS differences due to misalignment of the interferometers will be accounted for using the spectrum of HCl recorded with a lamp source and recorded simultaneously with the solar spectra using an internal gas cell included in all TCCON instruments.

The ILS describes the smearing of spectral line shapes in measured spectra due to the limited spectral resolution of the spectrometer. In the context of high-resolution Fourier transform infrared (FTIR) spectrometers, recorded spectra can be approximated by the convolution of the spectral irradiance with an ILS, as the ILS itself depends only weakly on wave number. The quantitative analysis of atmospheric spectra relies on a comparison of the measured spectra with simulated spectra. In an iterative procedure, relevant fit parameters are adjusted until a simulated spectrum converges to an observed spectrum. The simulation of spectra involves a radiative transfer model and spectral line lists, and includes instrumental effects such as the ILS. In order to generate data products of high precision and accuracy – as required for TCCON, since the variability of the target species is so low – significant deviations from the expected nominal ILS should be avoided and the residual deviations of the ILS from the expected shape should be carefully quantified. Typically, TCCON FTIR spectrometers are the high-resolution 125HR model manufactured by Bruker Optics, Germany. The nominal ILS of these spectrometers is determined by the maximum scan path, the solid angle covered by the interferometer's circular field stop, the wave number, and the numerical apodization function that is used (Davis et al., 2001). A successful alignment scheme for high-resolution spectrometers of the kind used in TCCON and the NDACC (Network for the Detection of Atmospheric Composition Change; Kurylo, 1991) was proposed about a decade ago and has become the standard alignment procedure for both networks (Hase and

Blumenstock, 2001). For the quantification of the residual deviations from the nominal ILS due to misalignment, optical aberrations and deviations from the nominal circular field stop, low-pressure gas cells are employed for ILS verification. The low-pressure gas inside the cell is chosen such that its absorption lines are preferably narrower than any spectral details observed in the atmospheric spectra. The FTIR network within the NDACC, which records spectra in the mid-infrared spectral region, uses HBr cells of 2 cm length filled with 2 mbar of HBr. These cells were provided by the National Center for Atmospheric Research (NCAR). More details on the HBr cell procedure and possible future enhancements are provided by Hase (2012) and references therein. TCCON uses 10 cm-long cells filled with 5 mbar of HCl, provided by Caltech (Washenfelder, 2006). Several cells of 20 cm length filled with 3 mbar of HCl are also in use. For the retrieval of the ILS from the gas cell spectra, the software LINEFIT is used in both networks (Hase et al., 1999).

Using sealed cells with compact cell bodies is advantageous because it provides a simple, very manageable method of ILS characterization. Choosing suitable gases allows constant monitoring of the cell in the solar beam for control purposes, although dedicated regular lamp measurements are regarded as indispensable for the most accurate ILS determination. The drawback of the compact cells is that it is not possible to attain sufficiently low pressures to achieve pure Doppler line shapes, as the observed absorption lines would then be too weak. Therefore, the spectral lines provided by the cells suffer from non-negligible pressure broadening. Although the lines are not significantly wider than Doppler-limited Gaussian lines in the chosen pressure range, the line shape is nonetheless sensitive to the amount of pressure in the cell. During the process of filling and sealing individual cells, deviations from the desired target gas column might arise. As long as these deviations are moderate (so that the spectral scene provided by each cell is similar), this is not an issue, as the retrieval of the ILS also retrieves the target gas column. The evaluator simply has to consider that the set of retrieved variables is self-consistent insofar as the retrieved column is compatible with the assumed partial pressure of the target gas, the cell length and cell temperature. However, even if we could rely on the assumption that the sealed cells contain pure gas, a calibration of the method is still required, as the assumed pressure broadening parameters or the band intensity may be incorrect, or the line shapes in the pressure range of a few mbar might be affected by narrowing effects (Dicke, 1953). This would introduce a systematic bias of the ILS parameters derived from a certain kind of cell.

Much more critical is the contamination of the cell content with other gases which remain undetected in the cell spectrum, e.g. due to intrusion of ambient air during the filling and sealing process. In this case, the actual total pressure in the cell exceeds the partial pressure of the target gas and results in an additional pressure broadening of the target gas lines. This additional broadening would – if it

remains unnoticed – be erroneously attributed to the ILS width. Moreover, this unnoticed contamination might vary from cell to cell. In that case, this problem would cause a station-to-station bias within the FTIR network, which would be much more detrimental than a common bias. Hase (2012) suggested a calibration method for the HBr cells used within NDACC by using refillable pressure-monitored N_2O cells in the 0.1 mbar pressure range. The proposed method is very robust because the nearby spectral signatures provided by the HBr and N_2O cells are observed in the same beam, so that any ILS imperfections of the spectrometer itself cancel out in the calibration process.

Here, we present a similar calibration scheme for the HCl cells used by TCCON. First, we investigate the impact of an ILS error on column-averaged dry air mole fractions of CO_2 (XCO_2) and derive target accuracies for the ILS knowledge and the HCl cell parameters. Next, we introduce the proposed method and describe the C_2H_2 reference cell used for the calibration. As a result of the calibration procedure, an effective pressure and target gas column is assigned to each cell. When a sealed HCl cell is used for operational ILS determination, this effective pressure is used for the line shape calculation instead of the pressure derived from the observed column, temperature and cell length. As the pressure inside a sealed cell is proportional to absolute temperature (unless the cell's gas column changes), the effective pressure for a mixture of ideal gases should behave in the same manner. Using a heated cell, we verify that this scaling law for the effective pressure allows us to retrieve consistent ILS parameters from a cell operated at different temperatures. Next, we estimate the precision and accuracy of the calibration method. Finally, we present results for a considerable set of HCl cells used in TCCON. We show that the cells have variable degrees of contamination (namely, that the ratio of the observed pressure broadening to the HCl column differs from cell to cell). The paper closes with a summary and an outlook on planned activities.

2 Propagation of ILS error into TCCON XCO_2

In this section, we investigate the sensitivity of TCCON XCO_2 data with respect to an error in the ILS width. This results in a requirement for the knowledge of the associated ILS parameters. Next, we quantify the impact of cell contamination on the ILS width as derived from HCl cell spectra. These considerations finally allow us to determine the acceptable amount of unnoticed contamination of the cell content, which increases the width of the target HCl lines used for the ILS retrieval.

FTIR spectrometers actually measure interferograms (which are converted into final spectra via the Fourier transformation), therefore it is an appealing approach to quantify and report the imperfections of the ILS in the interferogram domain (as the actual measurement process happens in the

optical path difference (OPD) domain). The LINEFIT software used for the ILS analysis within TCCON, retrieves a complex modulation efficiency (ME) as a function of OPD, which is represented by a ME amplitude and a ME phase error. The ME amplitude is related to the width of the ILS while the ME phase error quantifies the degree of ILS asymmetry. If the spectrometer meets the nominal ILS characteristics, the ME amplitude would be unity, and the ME phase error would be zero along the whole interferogram. Further details are provided by Hase (2012).

In the following, we quantify how the column-averaged dry-air mole fractions of CO_2 (XCO_2) reported by TCCON are affected by a deviation of the ME amplitude from unity. We do not treat the phase error/ILS asymmetry in the following, as the quantification of spectral line asymmetry is not critically affected by the assumed width of the HCl signatures provided by the cell. It is important to recollect that an XCO_2 result provided by TCCON is calculated from the ratio of CO_2 and O_2 columns derived from the same spectrum. This appealing strategy minimizes the error propagation of various instrumental and model errors into the reported dry-air mole fractions. For estimating the propagation of the ILS error, we apply a disturbance on the ME amplitude. The shape of this disturbance as a function of optical path difference is inspired by a common misalignment scenario due to a lateral shear offset of the interferometer's fixed cube corner (further details on this instrument-specific issue are provided by Hase, 2012). Correct error propagation needs to take into account that the misalignment affects both the CO_2 and O_2 , so it cancels out in XCO_2 to a large extent. However, because a wavefront error provoked by a given geometric displacement scales inversely with wavelength, the impact of a misalignment on ME amplitude increases with wave number, and is therefore smaller for CO_2 than O_2 (the wave number ratio between the O_2 and CO_2 bands used is 0.75). Note that the rise of ME amplitude beyond 1.0 does not indicate that the interferometer is more efficient than the ideal interferometer, rather this behaviour results from the fact that the ME amplitude is always normalized to 1.0 at zero path difference to ensure that the ILS is area-normalized in the spectral domain. In fact, when the ME amplitude rises above 1.0, the modulation is less than ideal at small OPD due to the assumed shear misalignment.

Figure 1 shows the assumed disturbances of the ME amplitudes for CO_2 and O_2 , taking the appropriate scaling law into account. The ME amplitude is shown up to 45 cm optical path difference, which is the recommended maximum optical path difference (OPD_{max}) applied within TCCON. We find that the induced column change depends slightly on the air mass. This result is not unexpected, as the signatures are not optically thin. Therefore, we quantified the effect for solar elevation angles of 30° and 60°. The change of the O_2 column amounts to 0.38 % (60°: 0.47 %), whereas the change in the CO_2 column is 0.46 % (60°: 0.54 %). The residual error in XCO_2 that is not compensated by ratioing

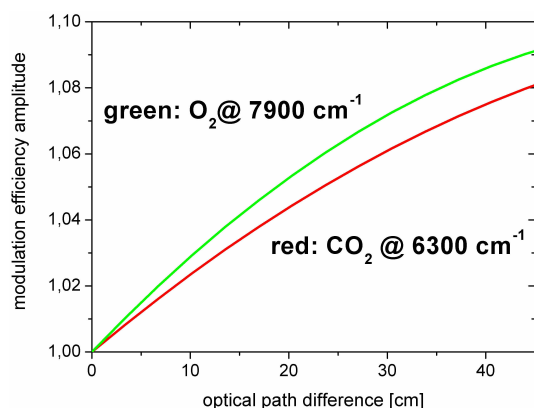


Fig. 1. Disturbance of ME amplitude assumed for characterization of TCCON XCO₂ product sensitivity with respect to ILS uncertainty. The wave number ratio of 0.8 between the CO₂ and O₂ bands used in the TCCON retrieval produces a shortening of the effective OPD by this same factor.

amounts to 0.07 % (~ 0.3 ppm) for the assumed ILS disturbance and does not significantly depend on the solar elevation. In the example, the ME amplitude disturbance at 45 cm OPD amounts to about 8 %. Therefore, we can estimate that the resulting error in XCO₂ is on the order of 0.035 % for a ME amplitude change of 4 % at OPD_{max}. The target station-to-station bias for the TCCON XCO₂ product is 0.1 %, hence – for ensuring that the ILS error is of secondary importance – we set a minimum performance metric for the error of the ME amplitude due to variations between HCl cells to be less than 4 %. This result is in excellent agreement with an earlier study performed by Griffith (2010).

In the current configuration, the retrieved ME amplitudes can change by 4 % at 45 cm OPD if the HCl pressure is in error by 0.5 mbar in the ILS retrieval setup. This requires that the description of the spectral line broadening should be correct within a range corresponding to a ± 0.25 mbar pressure interval of HCl for matching the requirements of the TCCON network performance. Since the self-broadening coefficients are larger than the air-broadening parameters by a factor of about four, the allowed pressure interval for the partial pressure of contaminating air would be accordingly larger. Nevertheless, for the sake of clarity, we determine and report in the course of the calibration procedure described in Sect. 4 only effective pressure parameters for a notional cell containing pure HCl (i.e. without ambient air or water vapour contamination). A separate treatment of self- and foreign broadening effects would require adjustments of two pressure values per cell. Such an extended approach would be complicated by uncertainties in the line parameters, by the fact that we work in a pressure region where the Voigt line shape model becomes questionable, and by the fact that we cannot safely assume that any of the investigated cells contains pure HCl. The only advantage of the extended approach would be that the

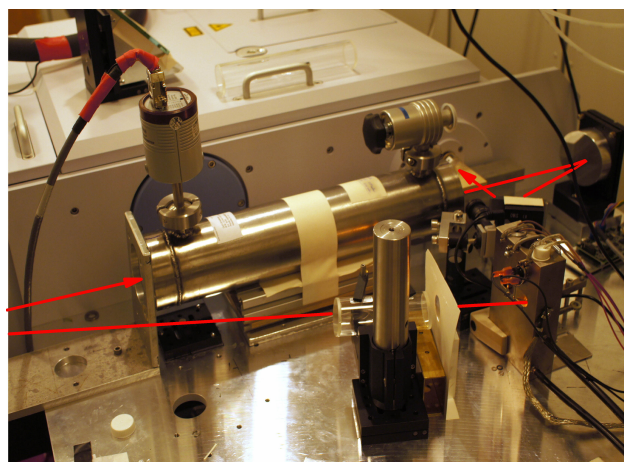


Fig. 2. Setup for HCl cell calibration at the TCCON site Karlsruhe. The source is on the right side in front, left from the source an HCl cell under test is located (protected by a heat shield to limit heating of the cell by the thermal radiation emitted by the source). The first mirror is on the left outside the figure. The long steel cylinder is the pressure-monitored C₂H₂ cell, the two mirrors in the rear right corner of the image steer the radiation into the spectrometer. The red arrow follows the radiation path from the global to the spectrometer input port.

resulting description of pressure broadening as a function of rotational quantum number might be slightly more realistic. However, using the simplified approach, we achieved nearly noise-limited fit residuals for all HCl cell spectra (signal-to-noise ratio around 2500), so we do not feel that the small benefits justify introducing this complication.

3 The pressure-monitored C₂H₂ reference cell

Our reference cell has 400 mm effective length, a free diameter of 70 mm and uses wedged CaF₂ windows. A precise capacitive pressure gauge with a 10 mbar working range is attached to the cell. The TCCON spectrometer in Karlsruhe is located in an air-conditioned container and is equipped with an optical board flanged to the spectrometer, which offers enough room for an external source, the reference cell and the cell under test. Three mirrors, one plane mirror, a 30° off-axis paraboloid, and a spherical mirror (used under a moderate off-axis angle) couple the beam into the spectrometer. Figure 2 shows the setup in front of the Bruker IFS125HR spectrometer. It should be noted that due to the use of wedged cell windows (in order to avoid channelling), the HCl cells noticeably impact the beam steering, so upon any cell exchange, the spherical mirror is slightly realigned in order to readjust the position of the source image on the field stop of the spectrometer.

The gas C₂H₂ offers a convenient band at 6550 cm⁻¹ in the vicinity of the CO₂ bands used for TCCON retrievals. Contrary to the mid-infrared, where a cell length of

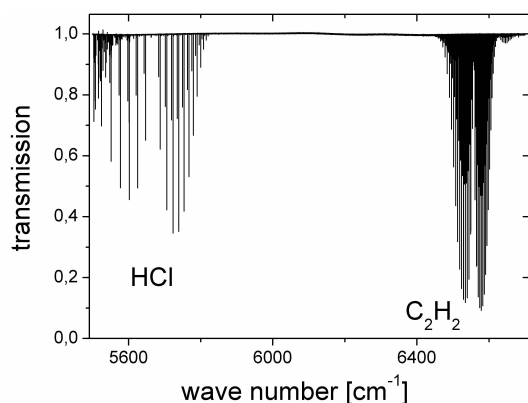


Fig. 3. Transmission spectrum recorded with the C_2H_2 and a TC-CON HCl cell in the beam. The band to the right is due to absorption by C_2H_2 , the band to the left is due to HCl absorption. Some H_2O signatures emerging in the lab air path can be detected at wave numbers below 5550 cm^{-1} .

even 200 mm is sufficient for generating strong N_2O lines with near-Gaussian line shape in the 0.1 mbar range, we have to use 3 mbar pressure to generate absorption lines of favourable strength. Figure 3 shows a measured spectrum, the C_2H_2 band can be seen in the right part of the figure, the HCl band on the left.

In order to minimize biases between the individual cell results, the same reference spectral scene (generated by the 400 mm cell filled with 3.00 mbar of C_2H_2 , measurements performed at temperatures in the range 291–294 K) is used for the calibration of all HCl cells. Nevertheless, as we do not work in the Doppler limit with the reference cell, it is appropriate to quantify the systematic bias of the calibration process due to C_2H_2 line shape issues, which is transferred into the HCl effective pressure parameters, as the derived values of these parameters rely on the ILS parameters derived from C_2H_2 . Therefore, we performed a pair of dedicated test measurements: the first measurement was performed with a reference cell filled with 3.00 mbar C_2H_2 and a TCCON HCl cell. The second measurement was performed with the same TCCON HCl cell in the beam and in addition two 400 mm reference cells in series, both reference cells were filled with 1.50 mbar of C_2H_2 . The discrepancy in the ILS parameters derived from C_2H_2 between both experiments reveals the systematic error of the method due to incorrect pressure broadening (and/or line strength) parameters of C_2H_2 and the applied Voigt line shape model. A sealed HCl cell (cell #1, see Sect. 6 and Table 1 for assignment of cell IDs) in the beam was added for detecting real alignment changes between the two experiments.

Figure 4 shows the reconstructed ME amplitudes for both setups. Indeed, the ME amplitudes derived from the HCl cell are in excellent agreement: the retrieved ME amplitudes differ by 0.3 % at 45 cm OPD. Therefore, we can assume that the alignment of the spectrometer did not change between

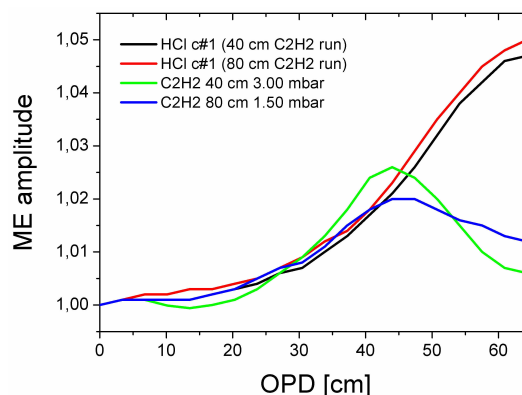


Fig. 4. ME amplitudes retrieved from a 40 cm cell filled with 3.00 mbar of C_2H_2 and two 40 cm cells in series, each filled with 1.50 mbar of C_2H_2 . For comparison, the ME amplitudes derived from an HCl cell (same cell was used for both measurements, effective cell parameters applied for ILS retrieval) are shown. The HCl results prove that the alignment status of the spectrometer did not change between the two measurements.

the measurements. The bump indicated in the 3.00 mbar C_2H_2 ME amplitude result is significantly dampened in the 1.50 mbar solution. In Sect. 5, we will use this discrepancy for an estimation of the systematic uncertainty inherent to the proposed HCl cell calibration method. All results indicate a moderate ME amplitude rise along the inner part of the interferogram, rising to values in the range of 2–2.5 % at 45 cm OPD (which is the OPDmax value recommended for TCCON). Beyond this OPD value, the HCl retrievals indicate a further pronounced increase, whereas the C_2H_2 analyses indicate a decrease of ME amplitude. It should be noted that the shape of the ME amplitude beyond 45 cm is reconstructed from minor details of the observed line shapes, so even very slight deficiencies of the line shape model affect the ME amplitude in this region of the interferogram. Measurements with a low-pressure N_2O cell taken with the same spectrometer (but using a different liquid-nitrogen cooled detector) in the mid-infrared region do not indicate such a pronounced rise of ME amplitude beyond 45 cm OPD. This indicates that the effect is most likely an artefact from the HCl cell itself (actual HCl line shape differs from assumed Voigt line shape), as probably is the ME bump at 45 cm observed in the ME amplitude derived from C_2H_2 . A very minor collisional narrowing effect acting on the spectral lines that is not included in the Voigt model will trigger an artificial increase in the reconstructed ME amplitude.

4 Calibration procedure for TCCON HCl cells

The calibration process of an HCl cell relies on a single lamp transmission spectrum. This spectrum is recorded with both the HCl cell to be tested and the 400 mm reference cell in the

Table 1. Calibration results for all investigated HCl cells. Abbreviations: CT: cell provided by California Institute of Technology, batch indicated in YYMM format; CT/NP: cell body provided by California Institute of Technology, but filled and sealed by company Neoplas, Greifswald, Germany; NP: cell body, filling and sealing by Neoplas.

Cell identifier, cell length in mm	Origin, batch, and location	Effective pressure H^{35}Cl at 296 K [hPa]	Effective pressure H^{37}Cl at 296 K [hPa]	HCl total column [$1\text{e}22\text{ molec/m}^2$] derived from H^{35}Cl	HCl total column [$1\text{e}22\text{ molec/m}^2$] derived from H^{37}Cl
1 (100)	CT1303 IMK-ASF	4.732	4.747	1.3133	1.3067
2 (100)	CT1303 IMK-ASF	4.702	4.683	1.3263	1.3195
3 (100)	CT1303 BIRA	5.111	5.119	1.3845	1.3781
4 (100)	CT1303 BIRA	5.070	5.056	1.3893	1.3828
5 (100)	CT1303 BIRA	4.949	4.979	1.3433	1.3384
6 (100)	CT1303 FMI	4.853	4.844	1.3415	1.3348
7 (100)	CT1303 FMI	4.863	4.890	1.3294	1.3253
8 (100)	CT1303 FMI	4.850	4.843	1.3262	1.3200
10 (100)	CT1303 FMI	5.127	5.147	1.4154	1.4094
11 (100)	CT1303 IUP Bremen	4.971	5.007	1.3247	1.3190
12 (100)	CT1303 IUP Bremen	4.997	5.022	1.3294	1.3232
13 (100)	CT1303 IUP Bremen	5.802	5.835	1.2967	1.2873
14 (100)	CT1303 IUP Bremen	4.830	4.880	1.3150	1.3103
15 (100)	CT1303 LPMAA/LERMA2*	4.964	4.991	1.3503	1.3458
16 (100)	CT1303 MPI-BGC	4.948	4.924	1.3450	1.3385
17 (100)	CT/NP0707 IMK-IFU	4.386	4.356	1.1932	1.1899
18 (100)	CT0805 (cell #G) Izana Observatory	5.070	5.133	1.2644	1.2567
19 (100)	CT0805 (cell #6) IUP Bremen	5.077	5.074	1.2729	1.2652
20 (100)	CT0805 (cell #3) IUP Bremen	5.578	5.603	1.2235	1.2170
35 (200)	CT 1304 IMK-ASF	3.147	3.123	1.6971	1.6870
36 (200)	CT1304 IMK-ASF	3.017	3.054	1.6375	1.6289
37 (200)	CT1304 NIWA	3.402	3.412	1.6541	1.6477
38 (300)	NP1012 NIWA	3.672	3.643	2.6070	2.6305

* The LPMAA laboratory will be included into the new LERMA2 laboratory infrastructure from January 2014 onwards.

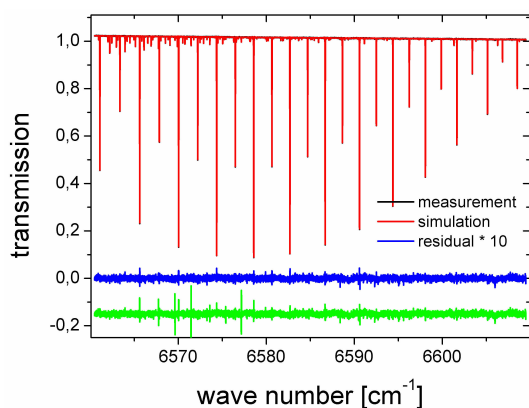


Fig. 5. Typical fit quality achieved for an ILS retrieval using C_2H_2 as described in Sect. 4. The green residual (vertically shifted for clarity) refers to the use of the original HITRAN 2008 line list.

beam, the latter filled with 3.00 mbar C_2H_2 , with the addition of an independent measure of the cell pressure. In order to achieve a spectral SNR on the order of 3000, eighty scans are recorded at a metering laser fringe scanning velocity of 20 kHz using a room-temperature InGaAs detector at a resolution of 0.014 cm^{-1} ($\text{OPD}_{\text{max}} = 64.3\text{ cm}$). The first step of the analysis process is to perform an ILS retrieval from the C_2H_2 band (spectral window: $6560.5\text{--}6609.5\text{ cm}^{-1}$) jointly with temperature. Figure 5 shows a typical C_2H_2 fit of ILS parameters. We essentially use the HITRAN 2008 (Rothman et al., 2009) line list for C_2H_2 , but corrected a few aberrant line positions. However, these modifications are essentially cosmetic interventions, and they negligibly affect the resulting ILS parameters. In the second step, a temperature retrieval is performed for the HCl band in the same spectrum. The consistency between the temperature retrievals from C_2H_2 and HCl is satisfactory: we do not find a significant bias and a standard deviation of about 0.3 K is achieved between the temperature values derived from HCl and C_2H_2 , respectively. Finally, we insert the ME result from C_2H_2 (and the temperature retrieved for the HCl cell) into a subsequent retrieval of HCl effective pressure (spectral window: $5172.0\text{--}5782.0\text{ cm}^{-1}$), again, from the same spectrum. As we observe signatures of both isotopologues H^{35}Cl and H^{37}Cl , we retrieve two effective pressure values. These effective pressure values and the HCl columns for both isotopologues comprise the final result of the cell calibration. If a repetition of the HCl temperature fit using these effective pressure values reveals a different temperature than retrieved in the previous step, the HCl analysis process is repeated until a final self-consistent solution is found. Note that for the determination of the effective pressure values, we exclusively use temperatures retrieved from the HCl band, as this procedure can be repeated at any TCCON site without the need for a temperature sensor on the cell body. Figure 6 shows a typical HCl

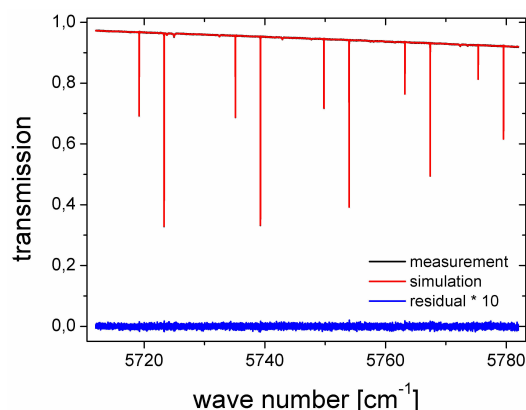


Fig. 6. Typical fit quality achieved after adjustment of the HCl effective pressure parameters (described in Sect. 4).

spectral fit. The original HITRAN 2008 spectroscopic line list for HCl is used without any modifications.

It is to be expected that the effective pressure parameters depend on temperature. Since the effective pressure affects the correction of the pressure broadening in the HCl cell, it is plausible to assume that it is proportional to the absolute temperature. Nevertheless, we want to check this assumption, as one might argue that the effective pressure is not actually a physical pressure value. Note that the procedure outlined in the following implicitly includes a test of whether the temperature dependence of the line-broadening parameters specified in HITRAN are compatible with our calibration approach. The test uses a pair of spectra from the same sealed HCl cell (cell #2), one spectrum is recorded at lab temperature (294.0 K), the other spectrum is recorded with the cell heated to 320.0 K. The C_2H_2 cell has been co-observed in both runs to ensure that the ILS was unchanged. The cell body of the HCl cell was wrapped with an electrical heating foil and an insulating foam film, such that only the window faces were in contact with the surrounding lab air. The cell temperature was monitored by a PT100 temperature sensor in contact with the cell body. The temperature value retrieved from the HCl band and the temperature value directly measured with the sensor are in good agreement for the measurement taken at lab temperature (retrieval: 294.66 K, sensor: 294.95 K), for the heated cell the retrieved temperature (319.87 K) is about 3 K lower than the sensor temperature (322.90 K). Due to the fact that the window faces were in contact with the ambient air, it is plausible that the temperature of the gas content is slightly lower than the temperature measured between the heating foil and the outer side of the cell body. The retrieved ME amplitudes are shown in Fig. 7 and are in reasonable agreement (1 % ME amplitude discrepancy at 45 cm OPD). Note that the temperature used in this test is further away from the calibration point (we performed the calibration measurements in the 291.0–294.0 K range) than we would expect to meet in practice, as the TCCON

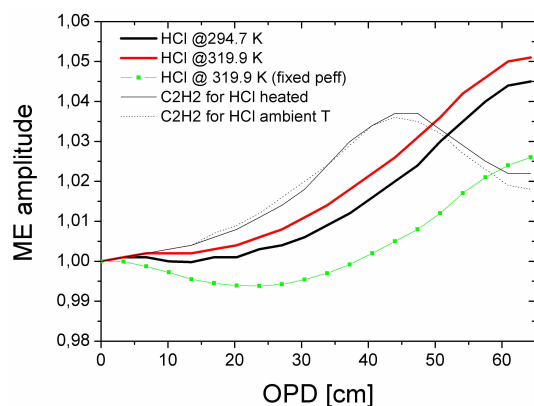


Fig. 7. ME amplitudes retrieved from HCl cell #2 at ambient temperature (black) and heated to about 320 K (red). The derived ME amplitudes are in good agreement under the assumption that the effective pressure values are proportional to absolute temperature. The ME amplitudes derived from C_2H_2 are also shown and prove that the alignment status of the spectrometer did not change. The dash-dotted green line would result if the effective pressure parameters were kept to their values at 294.7 K in the ILS analysis instead of converting them to the actual temperature.

spectrometers are typically operated under controlled conditions in laboratories or in air-conditioned containers.

Collecting all the procedural steps described in this section, the calibration can be summarized in the following step-by-step workflow: (1) a spectrum is recorded with both the reference cell and the HCl cell in the beam path. The 40 cm long and pressure-monitored reference cell is filled with 3 mbar of C_2H_2 . (2) A joint fit of ME and gas temperature is retrieved from the C_2H_2 lines, using the spectral window of $6560.5\text{--}6609.5\text{ cm}^{-1}$. (3) The resulting ME is adopted for the following analysis of the HCl spectrum. (4) The HCl pressure and gas temperature is retrieved using the spectral window of $5712.0\text{--}5782.0\text{ cm}^{-1}$. While the column amounts and pressure values are fitted individually for $H^{35}Cl$ and $H^{37}Cl$, a common value for the gas temperature is required. The resulting gas temperature is expected to agree with the temperature retrieved from C_2H_2 within a few tenths of a degree. (5) The final product of the calibration process are the effective pressure values at a reference temperature of 296 K and the column amounts for $H^{35}Cl$ and $H^{37}Cl$. (6) These effective pressure values replace the physical pressure values calculated from gas temperature, column amounts, and cell length in subsequent retrievals of ME of other spectrometers. If the gas temperature deviates from 296 K, the effective pressure values are converted to the actual temperature by assuming that the effective pressure is proportional to the absolute temperature.

5 Uncertainty characterization of the proposed calibration method

For an estimate of the precision of the calibration, we compare the effective pressure parameters for HCl cell #1, which have been determined three times in March, May, and June 2013. In between these measurements, interventions on the spectrometer were performed, e.g. a realignment and an exchange of the InGaAs detector element, so they cannot be regarded as a pure repetition of the identical measurement. The measurements were performed at retrieved cell temperatures of 291.3, 294.0, and 295.4 K. The scatter of the effective pressure (normalized to a reference temperature of 296 K) is 0.019 mbar for the main isotopologue $H^{35}Cl$, and 0.043 mbar for $H^{37}Cl$. This repeatability indicates that the precision of the method is well within the target precision of 0.25 mbar estimated in Sect. 2. The new calibration method is therefore accurate enough for safely eliminating any significant station-to-station bias due to ILS effects within TCCON target requirements.

For an estimate of the systematic bias of the calibration method due to deficiencies of the line shape model used for C_2H_2 , we compare the effective pressure parameters which result either from adopting the ME from the 1.5 mbar, 80 cm path length measurement presented in Sect. 3 or from adopting the ME from the 3.0 mbar, 40 cm standard setup. Using the 1.5 mbar ME instead of the 3.0 mbar ME reduces the effective pressure by 0.015 ($H^{35}Cl$) and 0.027 mbar ($H^{37}Cl$), respectively. The suspect ME amplitude bump at 45 cm OPD is damped by about a factor of 0.75 by halving C_2H_2 pressure. For estimating the full systematic bias, one possible assumption would be that a linear extrapolation of the observed ME amplitude change towards zero C_2H_2 pressure would provide the real ME. This assumption is motivated by the fact that in the zero pressure limit, the line shape converges to a pure Gaussian, and by the expectation that the spectral signal due to an incorrect line shape model is proportional to pressure in the low-pressure region. Under this assumption the observed amplitude change of the ME amplitude bump at 45 cm reveals half of the total effect (as we have made two measurements: the one using 3 mbar C_2H_2 pressure, which is the standard value we apply in the calibration procedure, and the other measurement performed for this sensitivity analysis, using 1.5 mbar pressure). As a consequence, the empirical numbers given above should be multiplied by a factor of 2 (and the ME amplitude bump as retrieved from C_2H_2 would be overestimated, but is not a spurious feature altogether). Following this line of argument, we can conclude that the systematic bias of the calibration method is 0.03 ($H^{35}Cl$) and 0.054 mbar ($H^{37}Cl$), respectively. An alternative – more pessimistic – assumption would be that the complete ME amplitude bump is an artefact of the C_2H_2 analysis. Under this assumption, we can estimate the effect by applying a modified ME amplitude without a bump for the retrieval of the HCl effective pressure parameters. Following this latter line

of argument, we can conclude that the systematic bias of the calibration method is 0.14 (H^{35}Cl) and 0.15 mbar (H^{37}Cl), respectively, which is still well within the target precision. Moreover, as stated before, this systematic bias propagates into the results of all calibrated HCl cells, so it can without difficulty be absorbed into the overall calibration factors applied in the TCCON network for matching the WMO reference (Wunch et al., 2010).

6 Results for TCCON HCl cells

Table 1 collects the results for all investigated HCl cells, namely the retrieved columns and effective pressure values for both isotopologues (referenced to a common temperature of 296.0 K). The cells with identifier #1–#16 belong to the same batch (effective cell body length of 100 mm); these cells were provided by the California Institute of Technology in spring 2013. This batch will be referred to as CT1303 (the batch identifier is explained in the caption of Table 1). Cells #18, #19, and #20 are from batches that were distributed by Caltech in earlier years. Cell #17 is a unique specimen, as the cell body has been provided by Caltech, but filling and sealing has been performed by a German company (Neoplas, Greifswald). In addition, we investigated three HCl cells with effective body lengths of 200 mm, recently distributed by Caltech (batch CT1304) and one cell of 300 mm length produced by Neoplas. Figure 8 shows the ratio of the effective pressure values resulting from the calibration to pressure values calculated from the observed HCl column. This ratio is – at least for cells with the same length and comparable HCl column – an accurate measure of HCl purity in the cell. The results for the weaker H^{37}Cl show slightly more scatter, but the consistency between the H^{35}Cl and H^{37}Cl is satisfactory and consistent with the precision estimation provided in Sect. 5. On average, the H^{37}Cl values are slightly smaller by 0.2 %, and the scatter of the difference between the two isotopologues is on the order of 0.026 mbar.

It is apparent that even the cells belonging to a common batch are not equivalent. For example, cell #13 seems to be significantly contaminated by foreign gases: for this cell the pressure broadening is 20 % larger than for the remainder of the CT1303 batch (we would like to emphasize here that the cell identifiers were assigned before the calibration spectra were analysed). The unique cell #17 shows similar performance to the majority of the cells in batch CT1303 (cell #13 excluded). The two cells, #18 and #19, distributed by Caltech in earlier years suffer from foreign gas contamination, showing about half of the excess broadening observed in cell #13. Cell #20 shows the highest amount of excess broadening among all tested cells. There are several more cells from this early batch in use that have yet to be characterized. Two of the new 200 mm cells, #35 and #36, are quite comparable with the majority of cells from the CT1303 100 mm cell batch. However, the third 200 mm cell, #37, of the CT1304

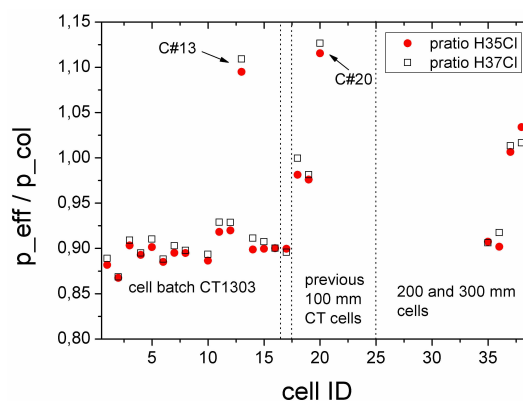


Fig. 8. The effective pressure values ratioed by pressure derived from observed column for the calibrated cells listed in Table 1. The dashed vertical lines separate different batches or different cell dimensions.

batch resembles the earlier cells #18 and #19. This is also the case for the Neoplas 300 mm cell #38.

The non-negligible scatter of effective pressure values found between the investigated cells underlines the value of the proposed calibration procedure. ILS retrievals from cell #13 or cell #20 without due consideration of the additional broadening would give rise to errors in the ME amplitude that exceed the criteria in Sect. 2 to meet TCCON requirements. Even the discrepancy between the earlier cells #18 and #19 and the remainder of the CT1303 batch would fail to meet these requirements. Since variability was found even within batches filled and sealed together, we suspect that subtle differences in cell handling procedures are significant at the level of precision desired for these calibrations. Potential sources of these subtle differences include the removal of water from the cell walls prior to the filling procedure and the leakage of air into the cell prior to cell sealing. In the out-gassing scenario, the reservoir of residual water in the cell depends on the amount of time the cell was evacuated prior to filling; in the air leakage scenario, the amount of air leakage depends on the integrity of the Teflon stopcock valve and the amount of time between filling and sealing. In both cases similar times were utilized for cells in the same batch, and pairs of cells were pumped and filled simultaneously. Nevertheless, variability is observed even among the paired cells. We note that water-broadening would be expected to be similar to self-broadening rather than air-broadening, such that the effect would be noticeable with relatively small amounts of residual water vapour.

Figure 9 shows a H_2O absorption line of useful intensity to reveal water vapour absorption inside the cell. This spectral window has been used to quantify the water vapour contamination in the HCl cells. The narrow dip observed at the line centre is due to absorption at low pressure, while the strong underlying absorption is generated in the lab air path. Unfortunately, the C_2H_2 reference cell might also suffer from some

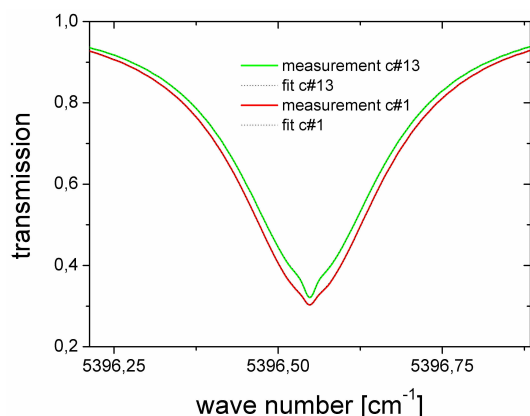


Fig. 9. A H_2O line as observed in a calibration measurement. The narrow dip observed at the line centre is due to absorption at low pressure, while the strong underlying absorption is generated in the lab air path. The superimposed dashed lines (which coincide with the solid lines at the resolution of the figure) are synthetic spectra generated with LINEFIT.

minor degree of H_2O contamination, so we can only quantify the total amount of water vapour in both cells from the available spectra (which were recorded with both the HCl cell undergoing testing and the reference C_2H_2 cell in the beam). However, the same C_2H_2 content was applied for the calibration of cells #1–#17. We might speculate that the lowest H_2O column observed within this sample actually resides in the C_2H_2 reference cell. Following this assumption, the H_2O column in the C_2H_2 cell was $9.9 \times 10^{20} \text{ molec m}^{-2}$. This column amount would correspond to a water vapour partial pressure of about 0.1 mbar in the 400 mm C_2H_2 cell body. Note that this is still not a relevant effect for the ILS determination from the reference cell, as it would result in 0.4 % ME amplitude change at 45 cm OPD, if we assume that line broadening by H_2O is twice as efficient as the C_2H_2 self-broadening. However, the analysis of a dedicated cell measurement using a mixture of 3 mbar of C_2H_2 and 7 mbar of H_2O indicates that the broadening of C_2H_2 lines by collisions with H_2O molecules is only 10 % more effective than self-broadening. Still, the calibration procedure would benefit from a proper quantification of H_2O contamination in the C_2H_2 cell, which will be included in future calibration runs. Figure 10 shows the effective pressure parameters as a function of the water vapour columns observed at low pressure. The water vapour column residing in the C_2H_2 cell causes a common offset of all data points towards higher abscissa values in this diagram. The data point in the upper right corner of the diagram refers to cell #13. The fact that the cell with the strongest additional broadening of the HCl lines in this sub-sample also suffers from the highest amount of water vapour supports the outgassing scenario. However, the retrieval of the water vapour amount inside the cells based on the weak

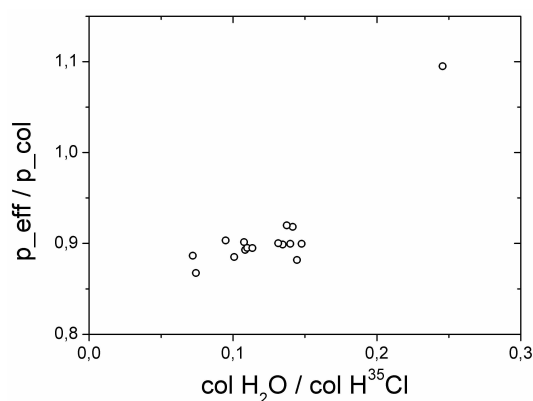


Fig. 10. The excess line broadening derived for H^{35}Cl as function of water vapour contamination for the cell batch CT1303. The data point in the upper right corner of the diagram refers to cell #13.

superimposed absorption dip shown in Fig. 9 is not accurate enough to exclude air leakage as an additional impact factor.

Although a discussion of spectroscopic data is outside the focus of this paper, we would like to point to the fact that the observed line widths for the purest cells are narrower than predicted by HITRAN 2008: the pressure broadening is about 12 % lower than expected. This might indicate that HITRAN 2008 reports incorrect band intensity or self-broadening coefficients for HCl, but as our measurements are performed in a pressure range that might be affected by narrowing effects, one should avoid drawing hasty conclusions. A new study of the HCl self-broadening and shift parameters is underway at JPL (Jet Propulsion Laboratory, California).

7 Summary and outlook

We have presented a novel, accurate method for calibrating the sealed HCl cells used by TCCON for ILS monitoring. We have applied the method to investigate a larger sample of cells and found non-negligible scatter of cell performance. We have derived effective cell parameters to ensure that all cells can be used for determining consistent ILS parameters. In the future, we plan to include all HCl cells that are used in TCCON and we will repeat the HCl cell characterization at regular intervals. The results will be collected and kept up-to-date by generating a table in the TCCON wiki. In addition, we will exploit the HCl column amounts determined for each cell in the course of the calibration for additional crosschecks of spectrometer performance within TCCON.

Acknowledgements. We would like to thank the head of the workshop at KIT IMK-ASF, A. Streili, for his exceeding commitment with the construction of the 40 cm cell bodies. We acknowledge support by the European integrating activity project InGOS (www.ingos-infrastructure.eu) for performing this study. BIRA thanks the Belgian Federal Science Policy for support through

the AGACC-II project. The LPMAA is grateful to the French INSU LEFE programme for supporting the TCCON-Paris project. Part of this work was performed at the Jet Propulsion Laboratory, California Institute of Technology, under contract with NASA. We acknowledge support by Deutsche Forschungsgemeinschaft and Open Access Publishing Fund of the Karlsruhe Institute of Technology.

The service charges for this open access publication have been covered by a Research Centre of the Helmholtz Association.

Edited by: D. Griffith

References

- Davis, S. P., Abrams, M. C., and Brault, J. W.: Fourier transform spectrometry, Academic Press, ISBN: 0-12-042510-6, 2001.
- Dicke, R. H.: The effect of Collisions upon the Doppler width of spectral lines, *Phys. Rev.* 89, 472–473, 1953.
- Dohe, S., Sherlock, V., Hase, F., Gisi, M., Robinson, J., Sepúlveda, E., Schneider, M., and Blumenstock, T.: A method to correct sampling ghosts in historic near-infrared Fourier transform spectrometer (FTS) measurements, *Atmos. Meas. Tech.*, 6, 1981–1992, doi:10.5194/amt-6-1981-2013, 2013.
- Griffith, D.: ILS sensitivity study by modulation-efficiency weighting of interferograms, Material presented on TCCON teleconference in January, 2010.
- Hase, F.: Improved instrumental line shape monitoring for the ground-based, high-resolution FTIR spectrometers of the Network for the Detection of Atmospheric Composition Change, *Atmos. Meas. Tech.*, 5, 603–610, doi:10.5194/amt-5-603-2012, 2012.
- Hase, F. and Blumenstock, T.: Alignment procedure for Bruker IFS 120 spectrometers, NDSC Infrared Working Group Meeting, Bordeaux, 2001.
- Hase, F., Blumenstock, T., and Paton-Walsh, C.: Analysis of the instrumental line shape of high-resolution Fourier transform IR spectrometers with gas cell measurements and new retrieval software, *Appl. Optics*, 38, 3417–3422, 1999.
- Keppel-Aleks, G., Wennberg, P. O., and Schneider, T.: Sources of variations in total column carbon dioxide, *Atmos. Chem. Phys.*, 11, 3581–3593, doi:10.5194/acp-11-3581-2011, 2011.
- Kurylo, M. J.: Network for the detection of stratospheric change (NDSC), SPIE Proceedings 1991, P. Soc. Photo-Opt. Ins., 1491, 168–174, 1991.
- Messerschmidt, J., Macatangay, R., Notholt, J., Petri, C., Warneke, T., and Weinzierl, C.: Side by side measurements of CO₂ by ground-based Fourier transform spectrometry (FTS), *Tellus B*, 62, 749–758, doi:10.1111/j.1600-0889.2010.00491.x, 2010.
- Miller, C. E., Crisp, D., DeCola, P. L., Olsen, S. C., Randerson, J. T., Michalak, A. M., Alkhaled, A., Rayner, P., Jacob, D. J., Suntharalingam, P., Jones, D. B. A., Denning, A. S., Nicholls, M. E., Doney, S. C., Pawson, S., Boesch, H., Connor, B. J., Fung, I. Y., O'Brien, D., Salawitch, R. J., Sander, S. P., Sen, B., Tans, P., Toon, G. C., Wennberg, P. O., Wofsy, S. C., Yung, Y. L., and Law, R. M.: Precision requirements for space-based X-CO₂ data, *J. Geophys. Res.-Atmos.*, 112, D10314, doi:10.1029/2006JD007659, 2007.
- Olsen, S. C. and Randerson, J. T.: Differences between surface and column atmospheric CO₂ and implications for carbon cycle research, *J. Geophys. Res.-Atmos.*, 109, D02301, doi:10.1029/2003JD003968, 2004.
- Rothman, L. S., Gordon, I. E., Barbe, A., Benner, D. C., Bernath, P. F., Birk, M., Boudon, V., Brown, L. R., Campargue, A., Champion, J.-P., Chance, K., Coudert, L. H., Dana, V., Devi, V. M., Fally, S., Flaud, J.-M., Gamache, R. R., Goldman, A., Jacquemart, D., Kleiner, I., Lacome, N., Lafferty, W., Mandin, J.-Y., Massie, S. T., Mikhailenko, S. N., Miller, C. E., Moazzen-Ahmadi, N., Naumenko, O. V., Nikitin, A. V., Orphal, J., Perevalov, V. I., Perrin, A., Predoi-Cross, A., Rinsland, C. P., Rotger, M., Simeckova, M., Smith, M. A. H., Sung, K., Tashkun, S. A., Tennyson, J., Toth, R. A., Vandaele, A. C., and Vander Auwera, J.: The HITRAN 2008 molecular spectroscopic database, *J. Quant. Spectrosc. Ra.*, 110, 533–572, 2009.
- Washenfelter, R. A.: Column abundances of carbon dioxide and methane retrieved from ground-based near-infrared solar spectra, PhD thesis, California Institute of Technology, Pasadena, California (available at: <http://thesis.library.caltech.edu>), 2006.
- Wunch, D., Toon, G. C., Wennberg, P. O., Wofsy, S. C., Stephens, B. B., Fischer, M. L., Uchino, O., Abshire, J. B., Bernath, P., Biraud, S. C., Blavier, J.-F. L., Boone, C., Bowman, K. P., Browell, E. V., Campos, T., Connor, B. J., Daube, B. C., Deutscher, N. M., Diao, M., Elkins, J. W., Gerbig, C., Gottlieb, E., Griffith, D. W. T., Hurst, D. F., Jiménez, R., Keppel-Aleks, G., Kort, E. A., Macatangay, R., Machida, T., Matsueda, H., Moore, F., Morino, I., Park, S., Robinson, J., Roehl, C. M., Sawa, Y., Sherlock, V., Sweeney, C., Tanaka, T., and Zondlo, M. A.: Calibration of the Total Carbon Column Observing Network using aircraft profile data, *Atmos. Meas. Tech.*, 3, 1351–1362, doi:10.5194/amt-3-1351-2010, 2010.
- Wunch, D., Toon, G. C., Blavier, J.-F. L., Washenfelter, R., Notholt, J., Connor, B. J., Griffith, D. W. T., Sherlock, V., and Wennberg, P. O.: The Total Carbon Column Observing Network, *Phil. T. Roy. Soc. A*, 369, 2087–2112, doi:10.1098/rsta.2010.0240, 2011.